

Supporting Information

Gap-tethered Au@AgAu Raman Tags for the Ratiometric Detection of MC-LR

Yuan Zhao,^{*,†} Fangjie Zheng,[†] Wei Ke,[†] Wei Zhang,[‡] Lixia Shi,[†] Han Liu[†]

[†]Key Laboratory of Synthetic and Biological Colloids, Ministry of Education, School of Chemical and Material Engineering, Jiangnan University, Wuxi, Jiangsu 214122, China.

[‡]Chongqing Institute of Green and Intelligent Technology, Chinese Academy of Sciences, Chongqing, 400714, China.

Corresponding author. E-mail: zhaoyuan@jiangnan.edu.cn

Table of Contents

Figure S1. (a) TEM image of Au NPs. (b) Statistical analysis of diameters for Au NPs.

Figure S2. Statistical analysis of gap size for Au@gap@AgAu NPs. (a) Au@gap@AgAu₍₁₎ NPs. (b) Au@gap@AgAu₍₂₎ NPs. (c) Au@gap@AgAu₍₃₎ NPs. (d) Au@gap@AgAu₍₄₎ NPs.

Figure S3. (a) Theoretically calculated optical absorption spectra of prepared Au@Ag@Au₍₂₎ NPs and Au@gap@AgAu₍₃₎ NPs. (b) Absorption spectra of prepared Au@Ag@Au NPs and Au@gap@AgAu NPs.

Figure S4. Raman spectra of Au@gap@AgAu₍₃₎ NPs using three different laser wavelengths.

Figure S5. (a) SERS spectra of 4-ATP molecules (from 10^{-7} M to 10^{-3} M) embedded in Au@gap@AgAu₍₃₎ NPs. (b) The plot of averaged Raman intensity at 1078 cm^{-1} with different concentrations of 4-ATP.

Figure S6. (a) Time-depending SERS spectra of GO/Fe₃O₄ NPs. (b) The corresponding RSD results of (a) calculated at 1305 cm^{-1} . (c) Plots of the SERS intensities of Au@gap@AgAu NPs-GO/Fe₃O₄ NPs assemblies at 1305 cm^{-1} (red points) and GO/Fe₃O₄ NPs at 1305 cm^{-1} (blue points) vs number of times.

Figure S7. (a) Magnetization curves of GO/Fe₃O₄ NPs, GO/Fe₃O₄ NPs after adding 13% HNO₃ and GO/Fe₃O₄ NPs after adding 30% H₂O₂. (b) Magnetic separation pictures of GO/Fe₃O₄ NPs after treatment with 13% HNO₃ and 30% H₂O₂.

Figure S8. I_{1078}/I_{1305} values with different stored time (a), different temperatures (b), different salt concentrations (c) and different pH values (d).

Table S1. The detail sequences of aptamers of MC-LR.

Table S2. Detection of MC-LR spiked in Tai lake water.

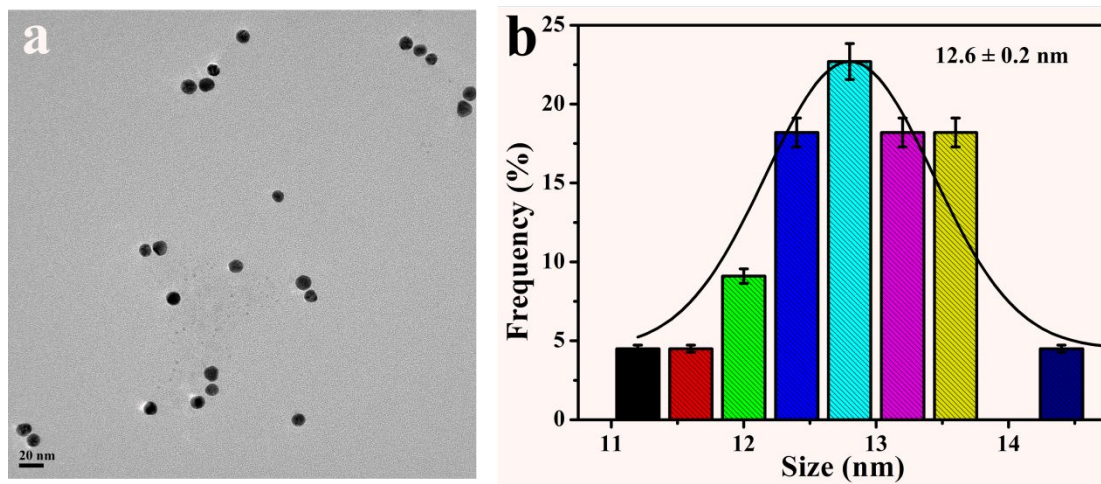


Figure S1. (a) TEM image of Au NPs. (b) Statistical analysis of diameters for Au NPs.

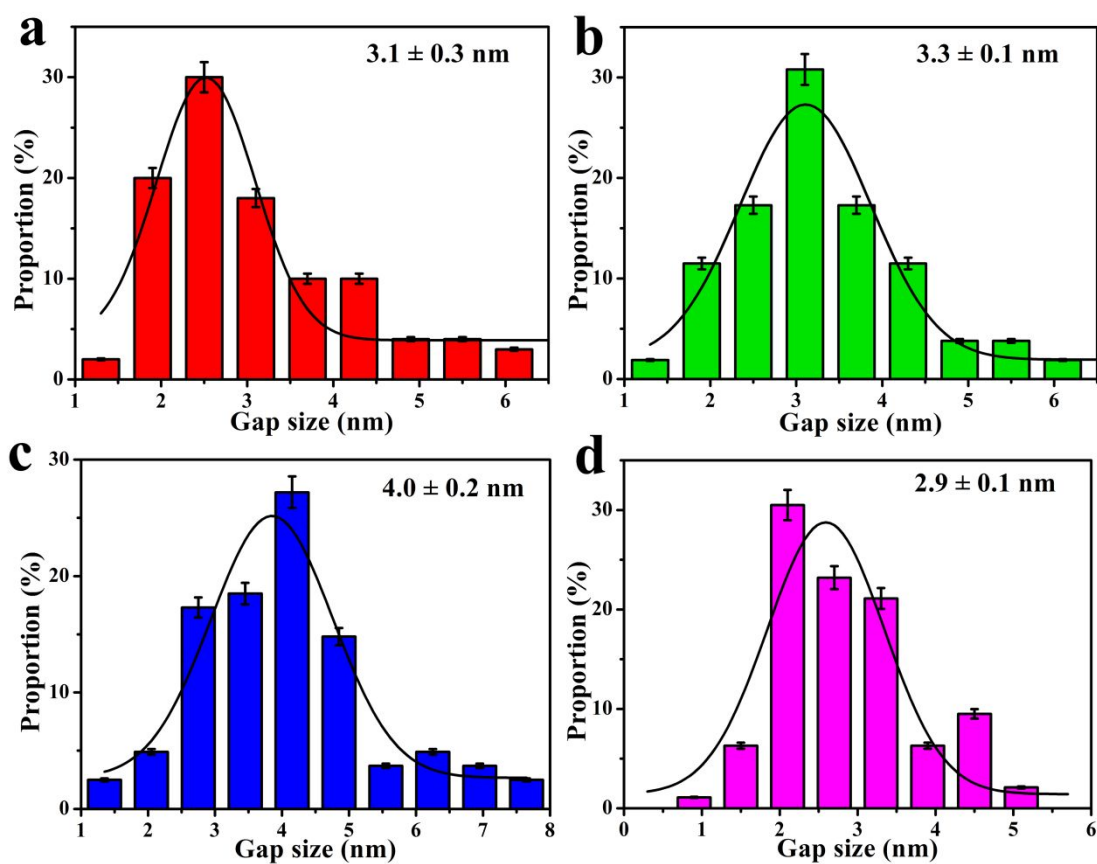


Figure S2. Statistical analysis of gap size for Au@gap@AgAu NPs. (a) Au@gap@AgAu₍₁₎ NPs. (b) Au@gap@AgAu₍₂₎ NPs. (c) Au@gap@AgAu₍₃₎ NPs. (d) Au@gap@AgAu₍₄₎ NPs.

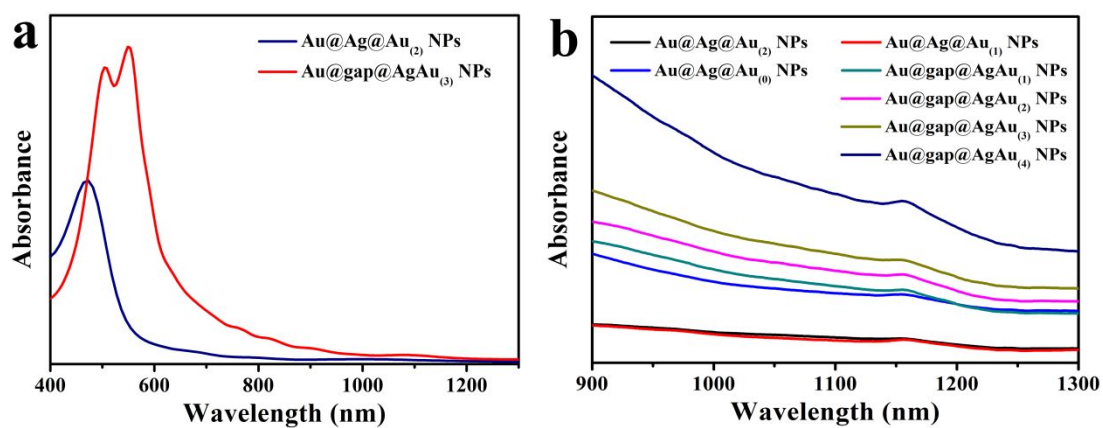


Figure S3. (a) Theoretically calculated optical absorption spectra of prepared $\text{Au@Ag@Au}_{(2)}$ NPs and $\text{Au@gap@AgAu}_{(3)}$ NPs. (b) Absorption spectra of prepared Au@Ag@Au NPs and Au@gap@AgAu NPs.

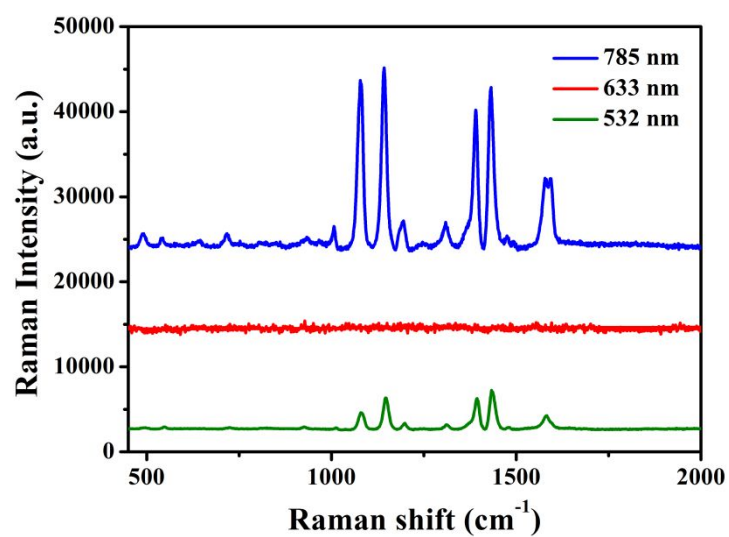


Figure S4. Raman spectra of Au@gap@AgAu₃ NPs using three different laser wavelengths.

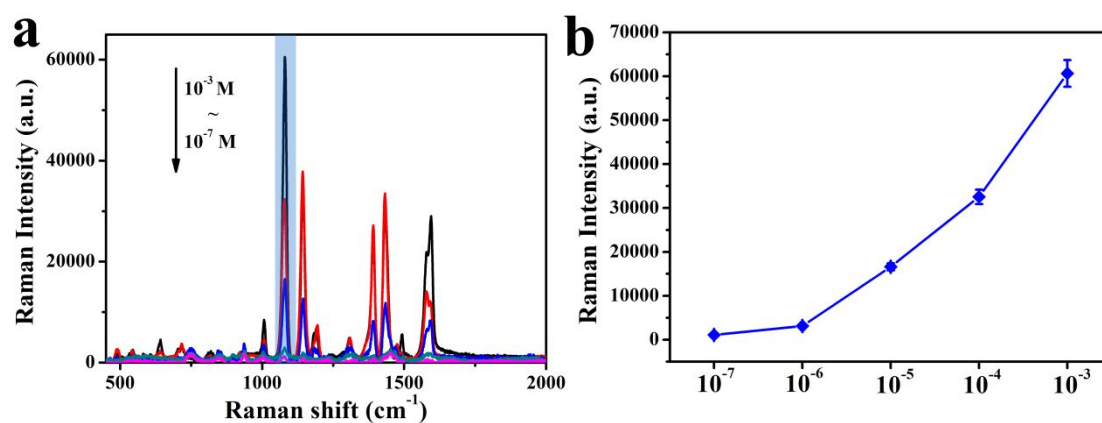


Figure S5. (a) SERS spectra of 4-ATP molecules (from 10^{-7} M to 10^{-3} M) embedded in Au@gap@AgAu₍₃₎ NPs. (b) The plot of averaged Raman intensity at 1078 cm^{-1} with different concentrations of 4-ATP.

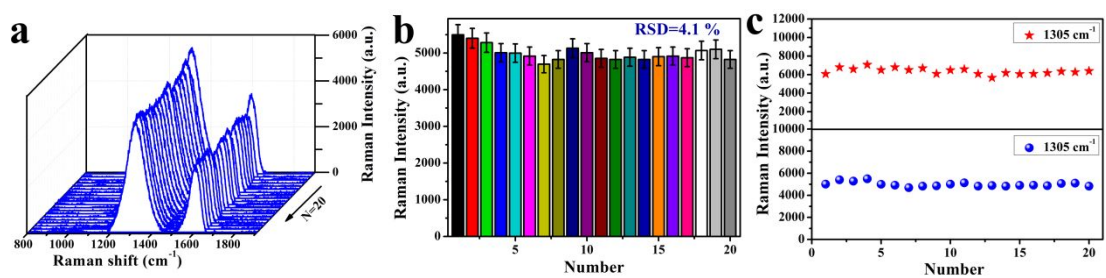


Figure S6. (a) Time-depending SERS spectra of GO/Fe₃O₄ NPs. (b) The corresponding RSD results of (a) calculated at 1305 cm⁻¹. (c) Plots of the SERS intensities of Au@gap@AgAu NPs-GO/Fe₃O₄ NPs assemblies at 1305 cm⁻¹ (red points) and GO/Fe₃O₄ NPs at 1305 cm⁻¹ (blue points) vs number of times.

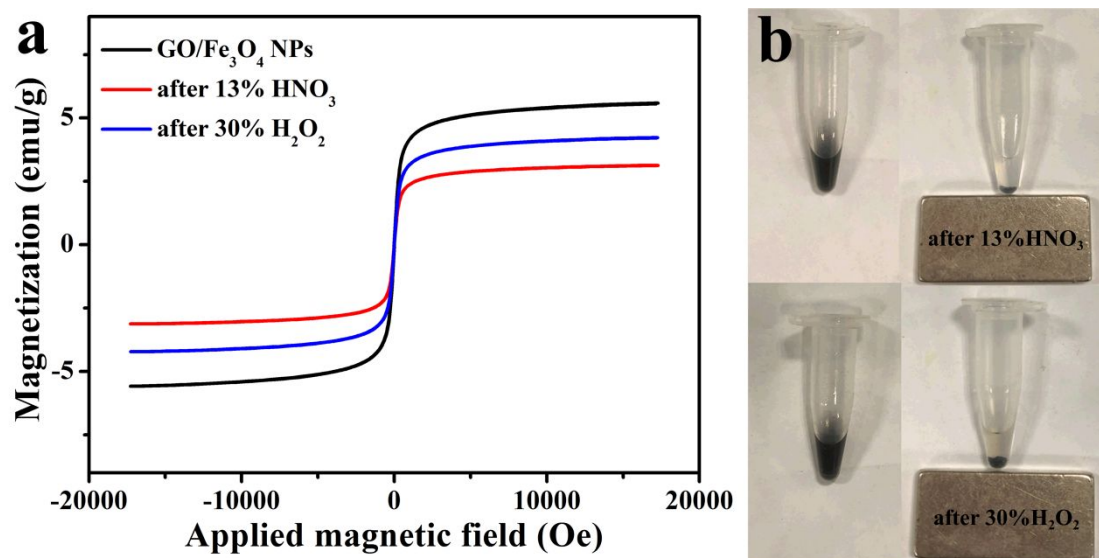


Figure S7. (a) Magnetization curves of GO/Fe₃O₄ NPs, GO/Fe₃O₄ NPs after adding 13% HNO₃ and GO/Fe₃O₄ NPs after adding 30% H₂O₂. (b) Magnetic separation pictures of GO/Fe₃O₄ NPs after treatment with 13% HNO₃ and 30% H₂O₂.

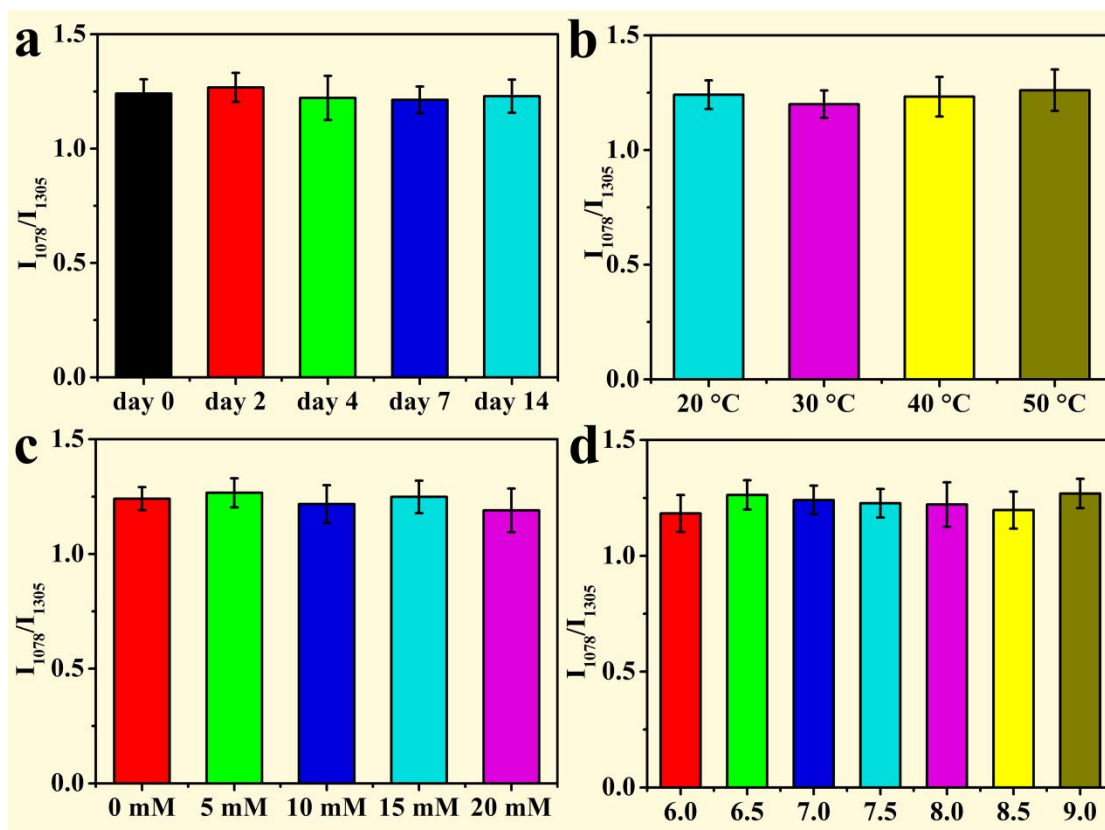


Figure S8. I_{1078}/I_{1305} values with different stored time (a), different temperatures (b), different salt concentrations (c) and different pH values (d).

Table S1. The detail sequences of aptamers of MC-LR.

Name	Sequences (5'-3')
Aptamers	-SH-GGC GCC AAA CAG GAC CAC CAT GAC AAT TAC CCA TAC CAC CTC ATT ATG CCC CAT CTC CGC

Table S2. Detection of MC-LR spiked in Tai lake water.

Polluted	Original	Spiked	Detected	Recovery
water	concentration	concentration	concentration	(mean± SD)
	(ng/mL)	(ng/mL)	(mean ± SD, ng/mL)	
1	0.39	0.25	0.61 ± 0.07	95.31 ± 2.65
2	0.27	0.5	0.76 ± 0.12	98.70 ± 3.36
3	0.62	2.5	3.05 ± 0.43	97.76 ± 3.07